Red-bond exponents of the critical and the tricritical Ising model in three dimensions

Youjin Deng[1,*] and Henk W. J. Blöte[1,2]
[1]*Faculty of Applied Sciences, Delft University of Technology, P. O. Box 5046, 2600 GA Delft, The Netherlands*
[2]*Lorentz Institute, Leiden University, P. O. Box 9506, 2300 RA Leiden, The Netherlands*
(Received 21 June 2004; published 24 November 2004)

Using the Wolff and geometric cluster algorithms and finite-size scaling analysis, we investigate the critical Ising and the tricritical Blume-Capel models with nearest-neighbor interactions on the simple-cubic lattice. The sampling procedure involves the decomposition of the Ising configuration into geometric clusters, each of which consists of a set of nearest-neighboring spins of the same sign connected with bond probability p. These clusters include the well-known Kasteleyn-Fortuin clusters as a special case for $p=1-\exp(-2K)$, where K is the Ising spin-spin coupling. Along the critical line $K=K_c$, the size distribution of geometric clusters is investigated as a function of p. We observe that, unlike in the case of two-dimensional tricriticality, the percolation threshold in both models lies at $p_c=1-\exp(-2K_c)$. Further, we determine the corresponding red-bond exponents as $y_r=0.757(2)$ and 0.501(5) for the critical Ising and the tricritical Blume-Capel models, respectively. On this basis, we conjecture $y_r=1/2$ for the latter model.

DOI: 10.1103/PhysRevE.70.056132 PACS number(s): 05.50.+q, 64.60.Cn, 64.60.Fr, 75.10.Hk

I. INTRODUCTION

Second-order thermodynamic transitions are generally accompanied by long-range correlations in both time and space. It is thus plausible that the precise microscopic structure of the system under consideration becomes unimportant as far as the universal aspects of the transition are concerned, and transitions in many different physical systems can be within the same universality class. It was suspected long ago [1–6] that, as indicated by the divergence of spatial correlation lengths, thermodynamic singularities near a critical point can be represented in terms of some sort of "geometric clusters." For instance, one may relate spontaneous long-range order below a critical temperature to the formation of an "infinite" cluster. As early as in 1967, Fisher [1] introduced a phenomenological droplet model for the two-dimensional Ising model, in which geometric clusters consist of nearest-neighboring (NN) Ising spins of the same sign. These clusters are referred to as Ising clusters, and topological considerations [7] the percolation threshold of the Ising clusters coincides with the thermal critical point of the Ising model two dimensions. This statement was further rigorously proved by Coniglio and co-workers [8]. However, it can also be shown [7] that Ising clusters are too "dense" to correctly describe critical correlations of the Ising model.

For the q-state Potts model (for a review, see Ref. [9]), which includes the Ising model as the special case $q=2$, a solution was given by Kasteleyn and Fortuin [10,11] in 1969. The Hamiltonian of a lattice Potts model with nearest-neighbor interactions only can be expressed as

$$\mathcal{H}/k_{\mathrm{B}}T = -K_p \sum_{\langle ij \rangle} \delta_{\sigma_i \sigma_j} \quad (\sigma = 1,2,\ldots,q), \tag{1}$$

where the sum $\langle\ \rangle$ is over all NN pairs, and K_p is the coupling constant. A correct geometric representation of this model can be obtained as follows. For each pair of NN spins in the same Potts state, a bond is placed with a probability $p_{\mathrm{KF}}=1-\exp(-K_p)$, such that the whole lattice is decomposed into groups of sites connected via the occupied bonds, which are known as the Kasteleyn-Fortuin (KF) clusters. The statistical weight of each bond-variable configuration is then given by the partition sum

$$Z(u,q) = \sum_b u^{n_b} q^{n_c} \quad (u = e^{K_p} - 1), \tag{2}$$

where the sum is over all bond-variable configurations, and n_b and n_c are the total numbers of bonds and KF clusters, respectively. As early as 1932, this partition sum had already appeared in the work of Whitney [13], and the corresponding model is referred to as the random-cluster model. It can be shown [9–11] that the random-cluster model can be exactly mapped onto the q-state Potts model. The percolation threshold of the former occurs [9–12] precisely at the thermal critical point in the latter. Scaling properties of KF clusters near criticality are governed by critical exponents of the Potts model (1). For instance, the fractal dimension of KF clusters at criticality is identical to the magnetic scaling dimension X_h. In fact, one may view the partition sum (2) as a generalization of the Potts model to noninteger q. It also includes some special cases such as $q \to 0$ and 1, where the latter reduces to the uncorrelated bond-percolation model [14]. It was because of the exact mapping between Eqs. (2) and (1) that Swendsen and Wang could develop [15] a cluster Monte Carlo method for the Potts model with integer $q=1,2,\ldots$. This method and its single-cluster version, the Wolff algorithm [16], significantly suppress the critical-slowing-down effect which is very prominent in the standard Metropolis method. Thus, these cluster algorithms have been extensively used in the field of critical phenomena and phase transitions.

The Potts model (1) includes the Ising model as a special case for $q=2$. For other values of q, one can, in the same way as for the Ising clusters defined earlier, form Potts clusters

*Present address: Laboratory for Material Science, Delft University of Technology, Rotterdamseweg 137, 2628 AL Delft, The Netherlands

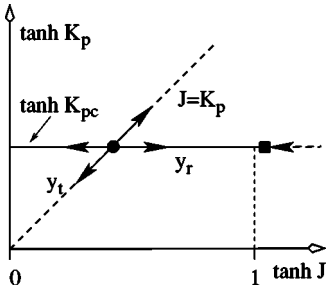

FIG. 1. Renormalization flow for the limit $s \to 1$ of the mixed Ising model described by Eq. (3) with $q=2$ in two dimensions. The dashed line $J=K_p$ is for the random-cluster representation of the Ising model, and arrows show the directions of renormalization flow.

[17–19] composed of NN sites in the same Potts state. As expected, these Potts clusters are also on average too "large" [20,21] to account for thermodynamic singularities of the Potts model. In the context of the renormalization group theory, this can be understood from a "mixed" Potts model, as described by [4,6]

$$\mathcal{H}/k_{\mathrm{B}}T = -J\sum_{\langle ij\rangle}(\delta_{\tau_i,\tau_j}-1)\,\delta_{\sigma_i\sigma_j} - K_p\sum_{\langle ij\rangle}\delta_{\sigma_i\sigma_j}. \qquad (3)$$

The second term is just the "pure" q-state Potts model (1); and the first term contains an auxiliary Potts variable $\tau=1,2,\ldots,s$. For the case that a pair of NN sites is in the same Potts state for both variables σ and τ, a bond is placed with the probability $p_{\mathrm{g}}=1-\exp(-J)$. As shown in Refs. [4] and [6] one can then express the partition sum of Eq. (3) in such bond variables, and differentiate the resulting free energy with respect to the parameter s, which is now regarded as a continuous variable. Taking the limit $s \to 1$, one obtains the size distribution of geometric clusters composed of NN sites in the same state σ connected with probability p_{g}. Thus, these clusters include KF and Potts clusters as two special cases for $J=K_p$ and $p_{\mathrm{g}}=1$, respectively.

The renormalization flow of the mixed Potts model (3) in two dimensions is schematically shown [21] in Fig. 1, where the dashed line $J=K_p$ represents the random-cluster model (2). Near the random-cluster fixed point $J=K_p=K_{pc}$, the renormalization flow along the dashed line is governed by the thermal exponent y_t of the Potts model. Further, on the critical line $K=K_{pc}$, the percolation threshold of geometric clusters occurs precisely at $J=J_c=K_{pc}$ [21]. The scaling field parametrizing the critical line near $J=K_{pc}$ is the bond-dilution field [6], and the associated exponent is called the red-bond exponent y_r. In contrast to the thermal and magnetic ones, the red-bond exponent y_r characterizes geometric properties of the Potts model, and does not have a thermodynamic analog. The scaling properties of geometric clusters with $p_{\mathrm{g}} > p_{\mathrm{KF}}(K_{pc})$, including Potts clusters, are governed by another fixed point, shown as the black square in Fig. 1. This fixed point is irrelevant ($y_r<0$) in the p_{g} direction, and we refer to it as the geometric-cluster fixed point [21]. For the two-dimensional Ising model on the square lattice, it occurs in the unphysical region $p_{\mathrm{g}}>1$ [19].

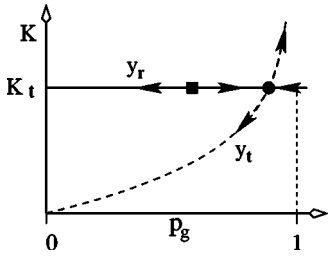

FIG. 2. Renormalization flow for the two-dimensional tricritical Blume-Capel model (4) with D fixed at the tricritical value D_t. The horizontal direction is the bond probability p_{g} in geometric clusters, and KF clusters are represented by the dashed line $p_{\mathrm{g}}=1-\exp(-2K)$.

However, the renormalization scheme in Fig. 1 is not generally valid [21] for two-dimensional models. For instance, we consider the two-dimensional Blume-Capel model [22] with the Hamiltonian

$$\mathcal{H}/k_{\mathrm{B}}T = -K\sum_{\langle ij\rangle} s_i s_j + D\sum_k s_k^2, \qquad (4)$$

where the spins can assume the values ± 1 and 0, and those in state $s=0$ are referred to as vacancies. The abundance of vacancies is controlled by the chemical potential D. For $D \to -\infty$, the vacancies are squeezed out, and the model (4) reduces to the spin-$\frac{1}{2}$ model. The critical coupling is an increasing function of D, and the critical line $K_c(D)$ terminates at a tricritical point (K_t, D_t). We mention that, for the Blume-Capel model (4), KF clusters should be constructed with the bond-occupation probability $p_{\mathrm{KF}}=1-\exp(-2K)$ instead of $p_{\mathrm{KF}}=1-\exp(-K)$, due to the difference between the Potts and the Ising Hamiltonians, as shown by Eqs. (1) and (4), respectively. For the case that the chemical potential D is fixed at the tricritical value D_t, the renormalization flow of the Blume-Capel model [21] is sketched in Fig. 2. The bond-dilution field near the random-cluster fixed point $p_{\mathrm{KF}}(K_t)$ is now *irrelevant* ($y_r<0$), and the percolation threshold p_{gc} of geometric clusters occurs at a *smaller* value than $p_{\mathrm{KF}}(K_t)$. Thus, at tricriticality (K_t, D_t), the thermodynamic singularities of the Blume-Capel model can be correctly represented by geometric clusters *as long as* the bond probability $p_{\mathrm{g}} > p_{\mathrm{gc}}$, including Ising clusters. It has been shown [21] that Fig. 2 applies to the whole tricritical branch of the Potts model in two dimensions.

As a result of exact solutions, Coulomb gas treatments [23], and conformal field theory [24], the critical behavior of the Potts model (1) is now well established in two dimensions. The exact values of a number of critical exponents are known. The geometric- and random-cluster fixed points in Figs. 1 and 2 were recently conjectured [21] to correspond with a pair of *critical* and *tricritical* Potts systems. These two models share the same conformal anomaly, and are related as $gg'=16$ in terms of the Coulomb gas coupling constant g [23].

For the three-dimensional Ising model, however, exact information is scarce, so that investigations have to depend on approximations, including Monte Carlo simulations as a

powerful tool. A considerable amount of research activity has been carried out [25–32]. For instance, there is some consensus that the thermal and magnetic exponents are $y_t=1.587$ and $y_h=2.482$, with uncertainties restricted to the last decimal place. Meanwhile, geometric properties of Ising systems have also received some attention [33–35]. For the spin-$\frac{1}{2}$ model on the simple-cubic lattice, infinite Ising clusters already exist even for zero coupling constant $K=0$. In the low-temperature phase $K>K_c$, infinite Ising clusters, composed of *minority* Ising spins, occur at about $1.05K_c$ [33–35], before the critical temperature is reached. However, in three dimensions, systematic investigations have not yet been reported about the renormalization flows in the parameter plane (K,p_g), as shown in Figs. 1 and 2. Particularly, it is not obvious whether or not the percolation threshold of geometric clusters on the critical line $K=K_c$ coincides with the random-cluster fixed point; and the red-bond exponent y_r remains to be determined.

In addition to the critical Ising model, the present paper also investigates the tricritical Ising model in three dimensions [36]. Since the upper tricritical dimensionality of $O(n)$ systems is *three*, exact information for some universal quantities is available, one of the rare cases in three dimensions. Exact values of critical exponents can be obtained from renormalization calculations [36] of the Landau-Ginzburg-Wilson Hamiltonian, and even from mean-field analyses. The leading and subleading thermal exponents [36] are $y_{t1}=2$ and $y_{t2}=1$, and the magnetic ones are $y_{h1}=5/2$ and $y_{h2}=3/2$, respectively. However, no exact results or numerical determinations for the red-bond exponent y_r have been reported to our knowledge; and it is even not obvious where the percolation threshold of geometric clusters occurs at tricriticality. It seems thus justified to perform a Monte Carlo investigation for the tricritical Ising model in three dimensions.

The organization of the remaining part of this paper is as follows. Section II reviews the simulation methods and defines the sampled quantities. The Monte Carlo data are analyzed in Sec. III, and Sec. IV presents a short discussion.

II. MONTE CARLO METHODS AND SAMPLED QUANTITIES

For simplicity, we chose the spin-$\frac{1}{2}$ and the tricritical Blume-Capel models as the subject of our simulations, so that the Hamiltonian of both models can be expressed by Eq. (4). The systems are defined on the $L\times L\times L$ simple-cubic lattice with periodic boundary conditions.

For the spin-$\frac{1}{2}$ model, as described by Eq. (4) for $D\to-\infty$, one can simply apply the Swendsen-Wang and Wolff cluster algorithms. In this case, the critical point on the simple-cubic lattice is known [32] as $K_c=0.221\,654\,55(3)$, where the number in parentheses is the error margin in the last decimal place. The finite-size analysis in Ref. [32] used a technique where Monte Carlo data for 11 Ising models were simultaneously fitted, such that universal parameters occur only once. In the present investigation, the precision of the above determination of K_c is considered to be sufficient.

However, for the general Blume-Capel model (4) in the presence of vacancies, the Swendsen-Wang or Wolff cluster simulations become incomplete, since they act only on Ising spins. In this case, the Metropolis method, which allows fluctuations of the vacancy density, can be used in combination with these cluster methods. Further, for the special case $D=2\ln 2$, a full-cluster simulation has also been developed [26,37] by mapping the system (4) onto a spin-$\frac{1}{2}$ model with two independent variables $\tau_1=\pm1$ and $\tau_2=\pm1$. Near tricriticality, however, no efficient cluster method is available so far to flip between vacancies and Ising spins. This problem was partly solved in Ref. [39] by means of the so-called geometric-cluster method [38]. This algorithm was developed on the basis of spatial symmetries, such as invariance under spatial inversion and rotation operations. It moves groups of Ising spins and vacancies over the lattice in accordance with the Boltzmann distribution, so that the magnetization and the vacancy density are conserved. We have used a combination of Metropolis, Wolff, and geometric steps, which significantly suppresses the magnitude of critical slowing down. Such simulations, together with other techniques such as the aforementioned simultaneous finite-size analysis, yield [39] the tricritical point as $K_t=0.7133(1)$ and $D_t=2.0332(3)$ on the simple-cubic lattice. The vacancy density ρ_v at the tricritical point is $\rho_v=\rho_{vt}=0.6485(2)$ [39]. These results are consistent with estimations [40,41] from other sources $K_t=0.706(4)$, $D_t=2.12(6)$, and $\rho_{vt}=0.652(6)$, within two times the error margins as quoted between parentheses.

In the present work, we used a constrained version of the Blume-Capel model described by Eq. (4), namely, the total number of vacancies is conserved while they are still allowed to move freely over the lattice. In this case, the chemical potential D in Eq. (4) becomes implicit, and a full-cluster simulation is realized by using a combination of Wolff and geometric cluster steps. It is known [39,42] that some tricritical singularities are strongly modified under this constraint. For instance, as already noted in Ref. [39], the constrained specific heat only reaches a finite cusp instead of being divergent at tricriticality. Nevertheless, the constraint does not lead to any change of the universality class, and the tricritical indices in the constrained and the unconstrained systems are exactly related. In particular, this constraint does not qualitatively influence phase diagrams such as Figs. 1 and 2. In comparison with the Blume-Capel model (4), simulations of its constrained version hardly suffer from critical slowing down even at the tricritical point. This is consistent with the Li-Sokal criterion [43] which specifies a lower limit for the dynamic exponent, since the constrained tricritical specific heat is finite [39]. Further, over a given number of samples, the statistical error margins of most quantities in the constrained system are much smaller than those in the unconstrained system, because the critical fluctuations are strongly suppressed for the former case.

The calculations in the present paper include two parts: the Monte Carlo simulations and the formation of geometric clusters with bond-occupation probability p_g. The latter step is performed as follows. For each pair of NN Ising spins of the same sign, a uniformly distributed random number r is drawn, and a bond is placed if $r<p_g$. This is done in an analogous way as in the well-known Swendsen-Wang proce-

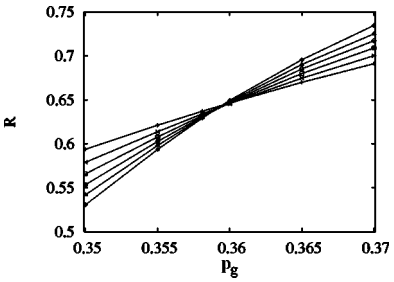

FIG. 3. Dimensionless ratio R for the critical spin-$\frac{1}{2}$ model in three dimensions, vs the bond probability p_g. The data points $+$, $\times$, $\square$, $\bigcirc$, $\triangle$, and $\diamond$ represent finite sizes $L=12$, 16, 20, 24, 28, and 32, respectively. The error margins of these data points are much smaller than the size of the above symbols. The clean intersection reveals that the location of the percolation threshold agrees with the random-cluster critical point.

dures. In this case, the whole lattice is decomposed into geometric clusters. The size of each cluster, defined as the total number of lattice sites in the cluster, is determined and used to calculate the quantities

$$l_2 = \frac{1}{N^2}\sum_i n_i^2 \quad \text{and} \quad l_4 = \frac{1}{N^4}\sum_i n_i^4, \tag{5}$$

where n_i is the size of the ith geometric cluster, and $N=L^3$ is the volume of the system. For KF clusters in which the bond probability $p_g=p_{KF}=1-\exp(-2K)$, it can be shown that the quantities in Eq. (5) are related to the magnetization m as

$$\langle m^2\rangle = \langle l_2\rangle \quad \text{and} \quad \langle m^4\rangle = 3\langle l_2^2\rangle - 2\langle l_4\rangle. \tag{6}$$

The first equality in Eq. (6) is derived as follows for the spin-$\frac{1}{2}$ model. We denote the numbers of plus and minus spins as N_+ and N_-, respectively, so that the total magnetization is $M=N_+-N_-$. Since all spins in a KF cluster are of the same sign, M can be written in terms of cluster sizes of KF clusters as $M=\Sigma_i n_i\tau_i$, where τ_i is the sign of spins in the ith cluster. The sign τ_i assumes $+1$ and -1 with equal probability, and is uncorrelated between different KF clusters. Thus, one has

$$m^2 = \frac{1}{N^2}\sum_i\sum_j n_i n_j \tau_i \tau_j = \frac{1}{N^2}\sum_i n_i^2. \tag{7}$$

The derivation of the second equality in Eq. (6) follows along similar lines.

On the basis of the quantities l_2 and l_4, we define a dimensionless ratio R as

$$R = \langle l_2\rangle^2/(3\langle l_2^2\rangle - 2\langle l_4\rangle), \tag{8}$$

which is equal to the magnetic ratio $Q=\langle m^2\rangle^2/\langle m^4\rangle$ for KF clusters, i.e., for $p_g=p_{KF}$. For the bond probability $p_g\neq p_{KF}$, R will be different from Q; its value reflects the geometric cluster size distribution. Further, the scaling behavior as a function of the distance p_g-p_{KF} is governed by the red-bond exponent y_r.

III. RESULTS

A. Spin-$\frac{1}{2}$ model

Simulations of the spin-$\frac{1}{2}$ model were performed at the critical point $K_c=0.221\,654\,55(3)$ [32], where the bond-occupation probability in KF clusters satisfies $p_{KF}(K_c)=1-\exp(-2K_c)=0.358\,091\,24(5)$. The system sizes were taken in the range $6\leqslant L\leqslant 48$, and we sampled the geometric quantities l_2, l_4, and R, and the magnetic ratio Q. Several Wolff cluster steps were carried out between consecutive sampling procedures. Part of the data for R is shown in Fig. 3, indicating that the percolation threshold of geometric clusters is near $p_{gc}\approx 0.358$, consistent with the random-cluster fixed point $p_{KF}(K_c)$. According to the least-squares criterion, we fitted the data for R by

$$R(p_g,L) = R_0 + \sum_{k=1}^{4} r_k[(p_g-p_{gc})L^{y_r}]^k + \sum_{j=1}^{3} a_j L^{y_j} + c(p_g-p_{gc})L^{y_1+y_r} + b(p_g-p_{gc})^2 L^{y_r}, \tag{9}$$

where R_0 is the universal number at p_{gc}. The terms with amplitudes r_k describe the effect of the bond-dilution field, and those with a_j account for finite-size corrections. We set the exponent $y_1=y_i=-0.821(5)$ [32], the leading irrelevant exponent of the three-dimensional Ising universality class. Other exponents of the correction terms, as described in Ref. [32], take values $y_2=d-2y_h=-1.964$ and $y_3=y_t-2y_h=-3.375$. The term with y_2 arises from the field dependence of the analytic part of the free energy, and that with y_3 is introduced by the nonlinear dependence of the thermal scaling field on the physical magnetic field. The term with amplitude c accounts for the "mixed" effect of the bond-dilution field and the irrelevant thermal field. The last term arises from nonlinear dependence of the bond-dilution field on the bond probability p_g. The data for Q were also included in the

TABLE I. The fit of the dimensionless ratio R for the critical spin-$\frac{1}{2}$ model in three dimensions. The numbers in parentheses are the statistical errors in the last decimal place.

y_r	p_c	R_0	r_1	r_2	r_3
0.757(2)	0.358 091 135(15)	0.6238(5)	−0.811(6)	−1.01(2)	−0.96(3)
r_4	a_1	a_2	a_3	b	c
4.5(5)	0.0965(3)	0.132(3)	1.2(8)	−0.35(2)	0.64(8)

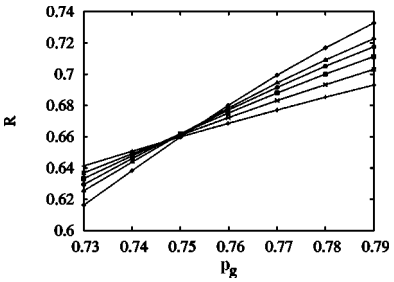

FIG. 4. Dimensionless ratio R for the tricritical Blume-Capel model in three dimensions, vs bond probability p_g. The data points $+$, $\times$, $\square$, $\bigcirc$, $\triangle$, and $\diamond$ represent finite sizes $L=8$, 16, 24, 32, 40, and 60, respectively. The error margins of these data points are much smaller than the size of the above symbols.

fit by Eq. (9) with $p_g=p_{KF}(K_c)$. Further, we included the Q data at K_c, published in Ref. [32]. These data, particularly those for larger system sizes $L=48$, 64, 128, and 256, were found very helpful in the numerical analysis. To obtain a satisfactory fit by Eq. (9) according to the least-squares criterion, it was necessary to discard the R data for small system sizes $L\leqslant 6$. We obtain $R_0=0.6238(8)$, $p_c=0.358\,091\,35(15)=p_{KF}(K_c)$, and $y_r=0.757(2)$, where the error margins are quoted as two standard deviations. The estimation of R_0 is in good agreement with the Binder ratio $Q=0.6241(4)$ [32]. We mention that, in Eq. (9), the contributions from the terms with b and c are significant. This is indicated by Table I, which lists detailed results of the above fit.

B. Tricritical Blume-Capel model

Using the Wolff and geometric cluster methods, we performed simulations of the Blume-Capel model at the estimated tricritical point $K_t=0.7133(1)$ and $\rho_{vt}=0.6485(2)$. Geometric clusters were formed among Ising spins, and we sampled l_2, l_4, R, and Q. The system sizes were taken in the range $6\leqslant L\leqslant 60$. For a finite system L at tricriticality, however, the total number of vacancies $L^3\rho_{vt}$ is not always an integer. Therefore, the actual simulations were performed at $[L^3\rho_{vt}]$ and $[L^3\rho_{vt}]+1$, where the brackets [ ] denote the integer part. The value of a sampled quantity at the tricritical point were obtained by a linear interpolation of the Monte Carlo data. For instance, we consider the dimensionless ratio R, and denote the R data at $[L^3\rho_{vt}]$ and $[L^3\rho_{vt}]+1$ as R_a and R_b, respectively. The tricritical value of R and its statistical error margin δR are then

$$R = xR_b + (1-x)R_a \quad \text{and} \quad \delta R = \sqrt{(x\,\delta R_b)^2 + [(1-x)\,\delta R_b]^2}, \tag{10}$$

respectively, where $x=L^3\rho_{vt}-[L^3\rho_{vt}]$.

At the tricritical point (K_t,ρ_{vt}), the bond probability at the random-cluster fixed point is $p_{KF}(K_t)=1-\exp(-2K_t)=0.7599(1)$. Part of the data for R is shown in Fig. 4, which indicates that the percolation threshold of geometric clusters also occurs at $p_{KF}(K_t)$. The data for R were fitted by

$$\begin{aligned} R(p_g,L) = R_0 + \sum_{k=1}^{4} r_k[(p_g-p_{gc})L^{y_r}]^k + a_1/\ln L + a_2/\ln^2 L \\ + a_3/L + a_4/L^2 + a_5/L^3 + b(p_g-p_{gc})L^{y_r-1} \\ + c(p_g-p_{gc})^2L^{y_r} + g(p_g-p_{gc})/L^2. \end{aligned} \tag{11}$$

The terms with amplitudes a_1 and a_2 account for logarithmic corrections [36] for the tricritical Ising model in three dimensions, as generally expected at borderline dimensionality of mean-field-like behavior. The last term in Eq. (11) arises from the field dependence of the analytical part of the free energy, where the factor $1/L^2$ is obtained as $L^{d-2y_{h1}}$ with $y_{h1}=5/2$ [36]. In analogy with the procedure for the spin-$\frac{1}{2}$ model, the Q data of Ref. [39] were included in the analysis for R with the corresponding bond probability $p_g=p_{KF}(K_t)$. After a cutoff for small system sizes $L<8$, we obtain $R_0=0.690(3)$, $y_r=0.501(3)$, and $p_g=0.759\,876(3)\approx p_{KF}(K_t)$. Detailed results are shown in Table II, which indicates that the amplitudes a_1 and a_2 for logarithmic corrections are rather small. Further, we observe that the result does not depend on whether the term with a_2 is included. Taking into account the uncertainties of the estimated tricritical point (K_t,ρ_{vt}), we obtain the red-bond exponent as $y_r=0.501(5)$.

As mentioned earlier, for the tricritical Ising model in three dimensions, exact values of a number of universal parameters, including the thermal and magnetic exponents, are known as integers or simple fractions [36]. Thus, on the basis of the numerical result $y_r=0.501(5)$, we *conjecture* that the red-bond exponent $y_r=1/2$ at the three-dimensional Blume-Capel tricritical random-cluster fixed point.

TABLE II. The fit of the dimensionless ratio R for the tricritical Blume-Capel model in three dimensions. The numbers in parentheses are the statistical errors in the last decimal place.

y_r	p_c	R_0	r_1	r_2	r_3
0.501(3)	0.759 876(3)	0.690(3)	−0.248(6)	−0.06(1)	0.08(3)
r_4	a_1	a_2	a_3	a_4	a_5
−0.2(2)	−0.0144(5)	0.04(4)	−0.227(5)	1.20(3)	−1.0(2)
a_5	b	c	g		
1.20(3)	4.2(5)	−0.40(5)	−2.8(3)		

IV. DISCUSSION

Using Monte Carlo simulations and finite-size analysis, we have investigated geometric properties of the critical Ising and tricritical Ising models in three dimensions. We find that the percolation threshold of critical geometric clusters occurs at the random-cluster fixed point, and the corresponding red-bond exponents are $y_r=0.757(2)$ and 0.501(5) for the above two models, respectively. Just like the thermal and magnetic exponents, the results of the red-bond exponent y_r apply to a large number of systems in the same universality class.

In comparison with the two-dimensional case, geometric properties of the tricritical Ising model are "qualitatively" different in three dimensions. In two dimensions, tricritical KF clusters are so "dense" [21] that the bond-dilution field becomes irrelevant near the random-cluster fixed point; the percolation threshold of geometric clusters occurs before $p_{\mathrm{KF}}(K_t)$, and belongs to a different universality class. In three dimensions, however, the red-bond exponent $y_r>0$ near $p_{\mathrm{KF}}(K_t)$, so that *only* KF clusters can correctly represent thermodynamic singularities near tricriticality.

As mention earlier, the red-bond exponent y_r describes geometric properties of the system under consideration, and does not have a thermodynamic analog. As a consequence, the exact value of y_r has not been obtained even for the tricritical Ising model in three dimensions. Although the conjecture $y_r=1/2$ is in agreement with the numerical determination $y_r=0.501(5)$, further investigations seem justified. For instance, one may ask the question whether one can derive y_r from mean-field-like considerations.

In addition to the red-bond exponent y_r, there are other geometric critical exponents, such as the fractal dimensions of "backbones" [44–46] and of "chemical" paths [47]. In the percolation theory, these exponents have received considerable attention and are considered to be of some physical relevance. For the $q\to 1$ Potts model, the red-bond exponent y_r just reduces to the thermal exponent y_t, which is about 1.14(2) in three dimensions [48].

ACKNOWLEDGMENTS

We are indebted to J. R. Heringa and X. F. Qian for valuable discussions. This research was supported by the Dutch FOM Foundation ("Stichting voor Fundamenteel Onderzoek der Materie") which is financially supported by the NWO ("Nederlandse Organisatie voor Wetenschappelijk Onderzoek").

[1] M.E. Fisher, Physics (Long Island City, N.Y.) **3**, 25 (1967).
[2] C.S. Kiang, D. Stauffer, and G.H. Walker, Phys. Rev. Lett. **26**, 820 (1971).
[3] K. Binder, Ann. Phys. (N.Y.) **98**, 390 (1976).
[4] A. Coniglio and W. Klein, J. Phys. A **12**, 2775 (1980); A. Coniglio and F. Peruggi, *ibid.* **15**, 1873 (1982); A. Coniglio, Phys. Rev. Lett. **62**, 3054 (1989).
[5] M.D. De Meo, D.W. Heermann, and K. Binder, J. Stat. Phys. **60**, 585 (1989).
[6] A. Coniglio, Nucl. Phys. A **681**, 451c (2001), and references therein.
[7] M.F. Sykes and D.S. Gaunt, J. Phys. A **9**, 2131 (1976).
[8] A. Coniglio, C.R. Nappi, F. Peruggi, and L. Russo, J. Phys. A **10**, 205 (1977).
[9] F.Y. Wu, Rev. Mod. Phys. **54**, 235 (1982).
[10] P.W. Kasteleyn and C.M. Fortuin, J. Phys. Soc. Jpn. **46** (Suppl.), 11 (1969).
[11] C.M. Fortuin and P.W. Kasteleyn, Physica (Amsterdam) **57**, 536 (1972).
[12] A. Coniglio and T.C. Lubensky, J. Phys. A **13**, 1783 (1980).
[13] H. Whitney, Ann. Math. **33**, 688 (1932).
[14] D. Stauffer and A. Aharony, *Introduction to Percolation Theory* (Taylor & Francis, Philadelphia, 1994).
[15] R.H. Swendsen and J.S. Wang, Phys. Rev. Lett. **58**, 86 (1987).
[16] U. Wolff, Phys. Rev. Lett. **62**, 361 (1989).
[17] A.L. Stella and C. Vanderzande, Phys. Rev. Lett. **62**, 1067 (1989).
[18] B. Duplantier and H. Saleur, Phys. Rev. Lett. **63**, 2536 (1989).
[19] H.W.J. Blöte, Y.M.M. Knops, and B. Nienhuis, Phys. Rev. Lett. **68**, 3440 (1992).
[20] C. Vanderzande, J. Phys. A **25**, L75 (1992).
[21] Y. Deng, H.W.J. Blöte, and B. Nienhuis, Phys. Rev. E **69**, 026123 (2004).
[22] M. Blume, Phys. Rev. **141**, 517 (1966); H.W. Capel, Physica (Amsterdam) **32**, 966 (1966).
[23] See e.g., B. Nienhuis, in *Phase Transitions and Critical Phenomena*, edited by C. Domb and J.L. Lebowitz (Academic, London, 1987), Vol. 11, p. 1.
[24] J.L. Cardy, in *Phase Transitions and Critical Phenomena* (Ref. [23]), p. 55.
[25] D.P. Landau, Physica A **205**, 41 (1994).
[26] H.W.J. Blöte, E. Luijten, and J.R. Heringa, J. Phys. A **28**, 6289 (1995).
[27] R. Guida and J. Zinn-Justin, J. Phys. A **31**, 8103 (1998).
[28] M. Hasenbusch, K. Pinn, and S. Vinti, Phys. Rev. B **59**, 11 471 (1999).
[29] For a review, see e.g., K. Binder and E. Luijten, Phys. Rep. **344**, 179 (2001).
[30] M. Campostrini, A. Pelissetto, P. Rossi, and E. Vicari, Phys. Rev. E **65**, 066127 (2002).
[31] Y. Deng and H.W.J. Blöte, Phys. Rev. Lett. **88**, 190602 (2002); Phys. Rev. E **67**, 066116 (2003).
[32] Y. Deng and H.W. J. Blöte, Phys. Rev. E **68**, 036125 (2003).
[33] H. Müller-Krumbhaar, Phys. Lett. **48A**, 459 (1974).
[34] D.W. Heermann and D. Stauffer, Z. Phys. B: Condens. Matter **44**, 339 (1981).
[35] A. Marro and J. Toral, Physica A **122**, 563 (1983).
[36] R.B. Stinchcombe, in *Phase Transitions and Critical Phenomena*, edited by C. Domb and J.L. Lebowitz (Academic, London, 1984), Vol. 7, p. 152.
[37] H.W.J. Blöte, L.N. Shchur, and A.L. Talapov, Int. J. Mod. Phys. C **10**, 1137 (1999).

[38] J.R. Heringa and H.W.J. Blöte, Physica A **232**, 369 (1996); Phys. Rev. E **57**, 4976 (1998).
[39] Y. Deng and H.W.J. Blöte, Phys. Rev. E **70**, 046111 (2004).
[40] S. Grollau, E. Kierlik, M.L. Rosinberg, and G. Tarjus, Phys. Rev. E **63**, 041111 (2001).
[41] M. Deserno, Phys. Rev. E **56**, 5204 (1997).
[42] M.E. Fisher, Phys. Rev. **176**, 257 (1968).
[43] X.J. Li and A.D. Sokal, Phys. Rev. Lett. **63**, 827 (1989).
[44] H.J. Herrmann and H.E. Stanley, Phys. Rev. Lett. **53**, 1121 (1984).
[45] P. Grassberger, Physica A **262**, 251 (1999), and references therein.
[46] Y. Deng, H.W.J. Blöte, and B. Nienhuis, Phys. Rev. E **69**, 026114 (2004).
[47] H.J. Herrmann, D.C. Hong, and H.E. Stanley, J. Phys. A **17**, L261 (1984).
[48] G. Paul, R.M. Ziff, and H.E. Stanley, Phys. Rev. E **64**, 026115 (2001).